Available online at www.sciencedirect.com
ScienceDirect
Trans. Nonferrous Met. Soc. China 19(2009) 72−77
Transactions of Nonferrous Metals Society of China
www.tnmsc.cn

In-situ dendrite reinforced Dy-based amorphous matrix composites

WU Xiao-feng(武晓峰), ZHAO Wei(赵 威), MENG Li-kai(孟力凯)

Faculty of Materials and Chemical Engineering, Liaoning University of Technology, Jinzhou 121001, China

Received 21 January 2008; accepted 19 May 2008

Abstract: In-situ dendritic reinforced Dy-Fe-Al amorphous matrix composites with a diameter of 3 mm were designed and fabricated by conventional Cu-mold casting method. XRD and SEM analyses were conducted to investigate the microstructure, the mechanical properties and the deformation and fracture behaviors of the composites. The forming mechanism and the deformation and fracture mechanism of the composites were discussed. The results indicate that the microstructures of composites consist of metallic glass matrix and α-Dy dendritic phase. The composites exhibit good mechanical properties with compressive fracture strength of 1 063 MPa, which is attributed to the effective bearing-load ability of the α-Dy dendrites and the glassy matrix and the restriction to the expanding of shear bands and cracks of the α-Dy dendrites. The nature of in-situ crystalline phases embedded in the amorphous matrix for in-situ crystallite reinforced Dy-Fe-Al amorphous matrix composites has a more important influence on the mechanical properties, the deformation and fracture behavior of the composites.

Key words: bulk metallic glasses(BMGs); composites; dysprosium(Dy); mechanical properties; deformation; fracture

1 Introduction

Since the first La-based bulk metallic glass(BMG) was prepared in 1989[1], rare-earth(RE) metal-based bulk metallic glasses(BMGs) have attracted a great deal of attention for their unique magnetic properties[2] and ultra-plasticity in supercooled liquid range[3]. However, these BMGs display low strength compared with other BMGs. For example, the highest compressive facture strength for La-based BMGs is 600 MPa[4], which is three times lower than that of Zr-based BMGs. In addition, there is significant difference in glass forming ability. The largest diameters of fully amorphous rods for La-based and Nd-based BMGs are close to 12 mm[5−6]. While for some RE-based BMGs, the diameter is less than 1 mm. Studies[4, 7−11] indicated that the composites consisting of in-situ precipitated dendritic or crystalline particle phases embedded in a glassy matrix exhibit enhanced compressive, occasionally tensile strength or plastic strain, which leads to significant improvement in impact toughness compared to monolithic BMGs. However, all of alloy systems selected in the studies such as Zr- and La-based alloys possess high glass forming ability. In order to expand alloy systems of the composites, Dy-based alloy has been chosen to design and prepare in-situ dendritic reinforced Dy-Fe-Al amorphous matrix composites by conventional Cu-mold casting method. The microstructure, mechanical properties and the deformation and fracture behavior of the composites are presented.

2 Experimental

Ingots with the nominal composition of $Dy_x(Fe_{0.6}Al_{0.4})_{100-x}$ (x=65, 70, 75, mole fraction) alloys were prepared by arc melting the mixture of pure metals (Dy, Fe and Al) with a purity of more than 99.9% under a Ti-gettered Ar atmosphere. To ensure homogeneity of the samples, the ingots were remelted several times. 50 mm long cylindrical rods with a diameter of 3 mm were prepared by pouring liquid metal which was melted using induction furnace through a quartz nozzle into a copper mold under certain argon pressure as well as purified argon atmosphere. The microstructure of the samples was detected by X-ray diffractometry(XRD) using a Rigaku X-ray diffractometer (Cu K_α radiation). Compression experiments were carried out on a MTS-type axial-torsional load frame at room temperature. The samples with an aspect ratio of 2:1 were prepared for the

Foundation item: Project(20032137) supported by the Natural Science Foundation of Liaoning Province, China
Corresponding author: WU Xiao-feng, Tel: +86-416-4199758; E-mail: hgd901@126.com
DOI: 10.1016/S1003-6326(08)60231-9

compressive testing. The compressive strain rate used was 3.0×10^{-4} s^{-1}. Six rods with the same diameter and composition were compressed. The microstructures were examined by an optical microscope. JEOLJSM6301 scanning electron microscope(SEM) was used for the analysis of the as-cast morphologies and fracture features. SEM electron microprobe analysis was used to determine the average compositions of the main phases.

An indentation experiment was performed on a HV-1000-type microscopic hardness tester. A diamond indentor was used. The indentor was loaded under 5 N and the maximum load for 10 s. The indented morphology was observed on optical microscope.

3 Results

3.1 Phase constitutions and microstructure

Fig.1 shows the XRD patterns of the cast 3 mm diameter rods of $Dy_x(Fe_{0.6}Al_{0.4})_{100-x}$ (x=65, 70 and 75) alloys. The XRD patterns of the alloys show some crystalline peaks superimposed on amorphous maximum, indicating the formation of an amorphous/crystalline composite structure. The crystalline phase existing in the three alloys was identified as β-Dy, a high temperature phases, and the other two crystalline phases were identified as α-Dy existing in $Dy_{70}(Fe_{0.6}Al_{0.4})_{30}$ and $Dy_{75}(Fe_{0.6}Al_{0.4})_{25}$ and AlFeDy ternary intermetallics existing in $Dy_{65}(Fe_{0.6}Al_{0.4})_{35}$, respectively.

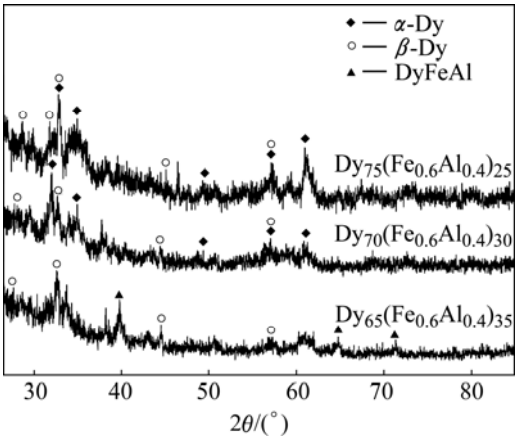

Fig.1 XRD patterns of $Dy_x(Fe_{0.6}Al_{0.4})_{100-x}$ (x=65, 70, 75) alloys

Fig.2 shows the optical micrographs obtained from the cross section of as-cast $Dy_x(Fe_{0.6}Al_{0.4})_{100-x}$ with a diameter of 3 mm. The microstructure of $Dy_{65}(Fe_{0.6}Al_{0.4})_{35}$ consists of white net-like phase and a few dark particles embedded in a gray glassy matrix (Fig.2(a)). EDX analysis indicates that the net-like phase is enriched in Fe and Al, the particles are enriched in Dy and a few other elements are included in the particles compared with the overall alloy composition. Combined with the XRD patterns, the net-like phase and the particles

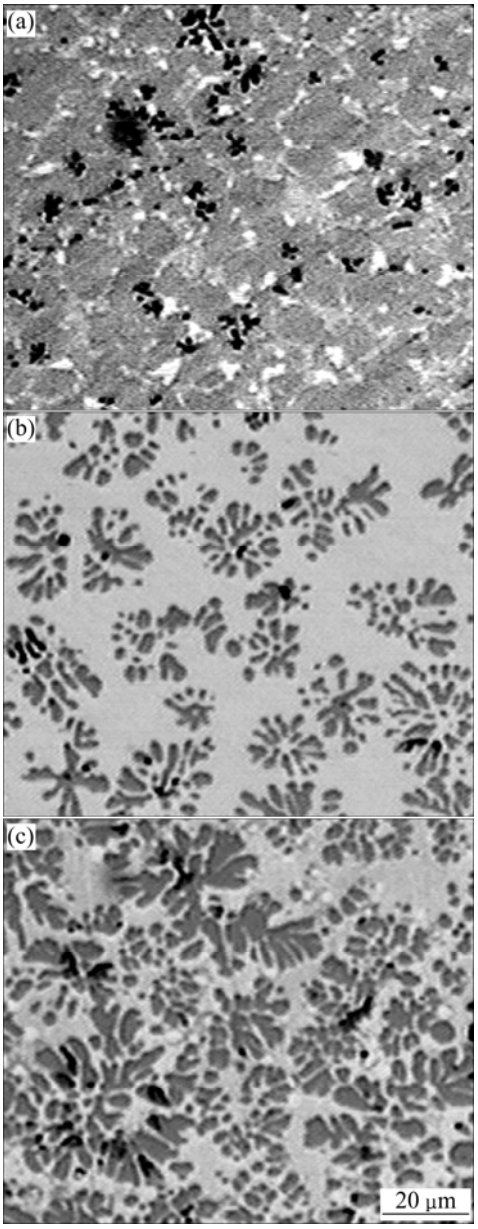

Fig.2 Optical micrographs of $Dy_{65}(Fe_{0.6}Al_{0.4})_{35}$ (a), $Dy_{70}(Fe_{0.6}Al_{0.4})_{30}$ (b) and $Dy_{75}(Fe_{0.6}Al_{0.4})_{25}$ (c)

are determined to be ternary AlFeDy intermetallic and β-Dy.

For $Dy_{70}(Fe_{0.6}Al_{0.4})_{30}$ and $Dy_{75}(Fe_{0.6}Al_{0.4})_{25}$, different microstructures are obtained as shown in Figs.2(b) and (c). Flower-like dendritic phase and a few dark particles disperse in a gray glassy matrix. From the XRD patterns and EDX analysis, the dendritic phase and the particles are determined to be α-Dy and β-Dy, respectively. The volume fraction of the β-Dy in the two alloys is almost the same, namely, 6.3% (volume fraction) for $Dy_{70}(Fe_{0.6}Al_{0.4})_{30}$ and 6.8% for $Dy_{75}(Fe_{0.6}Al_{0.4})_{25}$, respectively. However, α-Dy phase is different and 41.5% for $Dy_{70}(Fe_{0.6}Al_{0.4})_{30}$ and 62.3% for $Dy_{75}(Fe_{0.6}Al_{0.4})_{25}$, respectively. From the optical

micrographs of $Dy_{70}(Fe_{0.6}Al_{0.4})_{30}$ (Figs.2(b) and (c)), it is also seen that α-Dy dendrites are uniformly dispersed throughout the glassy matrix.

3.2 Compressive properties

A series of compression tests were conducted on three as-cast Dy-based alloys. Fig.3 shows the quasistatic compressive stress—strain curves at room temperature for the as-cast $Dy_x(Fe_{0.6}Al_{0.4})_{100-x}$ rods with a diameter of 3 mm and a length of 6 mm. Like other metallic glasses, the curves of the three alloys only display an initial elastic deformation behavior with almost no plasticity at room temperature. However, there is a significant difference in the values of fracture strength. The fracture strength of $Dy_{65}(Fe_{0.6}Al_{0.4})_{35}$ is only 420 MPa, while that of the $Dy_{70}(Fe_{0.6}Al_{0.4})_{30}$ and the $Dy_{75}(Fe_{0.6}Al_{0.4})_{25}$ reach 1 063 MPa and 960 MPa, respectively, which is 400 MPa larger than that of the La-based BMGs and their composites[4]. To our knowledge, this is the highest for RE-based BMGs and their composites reported so far.

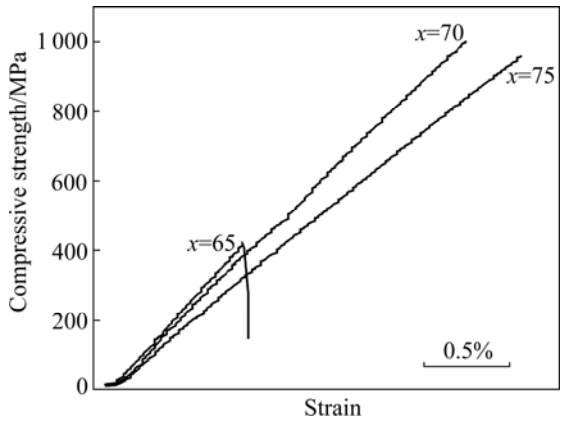

Fig.3 Stress—strain curves of $Dy_x(Fe_{0.6}Al_{0.4})_{100-x}$ (x=65, 70, 75) alloys

3.3 Fracture morphology

Fig.4 shows the morphologies of the fractured specimen of the three alloys under uniaxial compressive loading. The $Dy_{65}(Fe_{0.6}Al_{0.4})_{35}$ shatters into two fragments longitudinally easily (Fig.4(a)), and the direction is parallel to the compressive loading axis during compressive test. In contrast, the fracture of $Dy_{70}(Fe_{0.6}Al_{0.4})_{30}$ and $Dy_{75}(Fe_{0.6}Al_{0.4})_{25}$ occurs in a shear mode, as seen in Figs.4(b) and (c). The compressive fracture surface is inclined under an angle θ to the stress axis and can be measured as marked in the figures. The fracture angles θ between the stress axis and the fracture surface (shear plane) are equal to 41° for $Dy_{70}(Fe_{0.6}Al_{0.4})_{30}$ and 43° for $Dy_{75}(Fe_{0.6}Al_{0.4})_{25}$, respectively, indicating the dominance of shear stress in the failure process.

Fig.5 shows the micrograph of the fracture surfaces of the three alloys. $Dy_{65}(Fe_{0.6}Al_{0.4})_{35}$ fractures in brittle features with some angular crystals dispersing in a rough rock-layer matrix. Some cracks can be seen in the crystals and the matrix. The cracks in the matrix pass through the angular crystals (Fig.5(a)). $Dy_{70}(Fe_{0.6}Al_{0.4})_{30}$ exhibits a very different fracture surface (Fig.5(b)), on which a vein pattern can be observed. The veins take a direction from right to left as marked by arrows. This is consistent with shear sliding and fracture of the whole sample. Also, it can be noticed that local melting as evidenced by the formation of "liquid droplets" takes place during loading (Fig.5(c)). These phenomena appear very often in monolithic BMGs. Compared to BMGs, however, the veins are undeveloped and the fracture surface is like a slurry flow (Fig.5(b)). In addition, the liquid droplets are larger (Fig.5(c)). This appears that the dendritic phases embedded in the glassy matrix make the temperature in the shear band become higher enough to

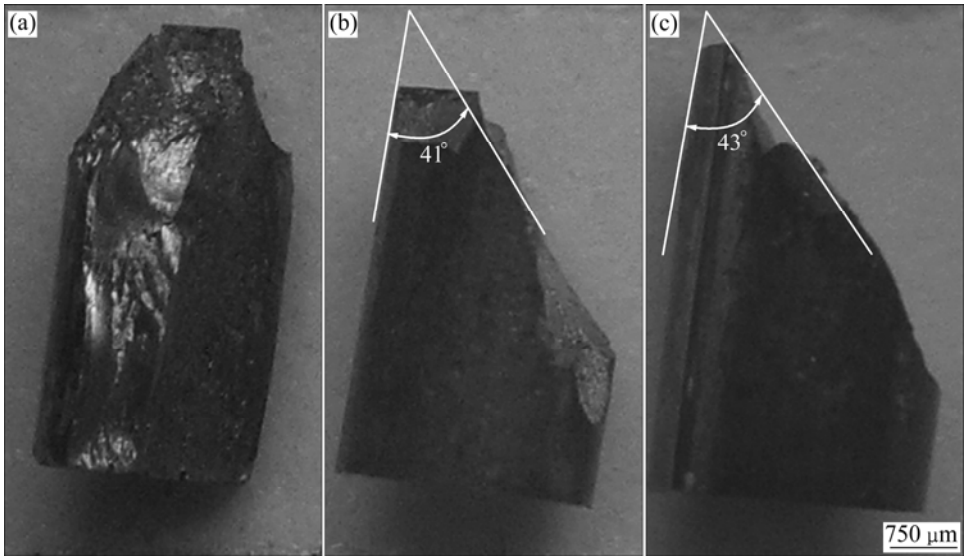

Fig.4 Macroscopic fracture surfaces of $Dy_{65}(Fe_{0.6}Al_{0.4})_{35}$ (a), $Dy_{70}(Fe_{0.6}Al_{0.4})_{30}$ (b) and $Dy_{75}(Fe_{0.6}Al_{0.4})_{25}$ (c)

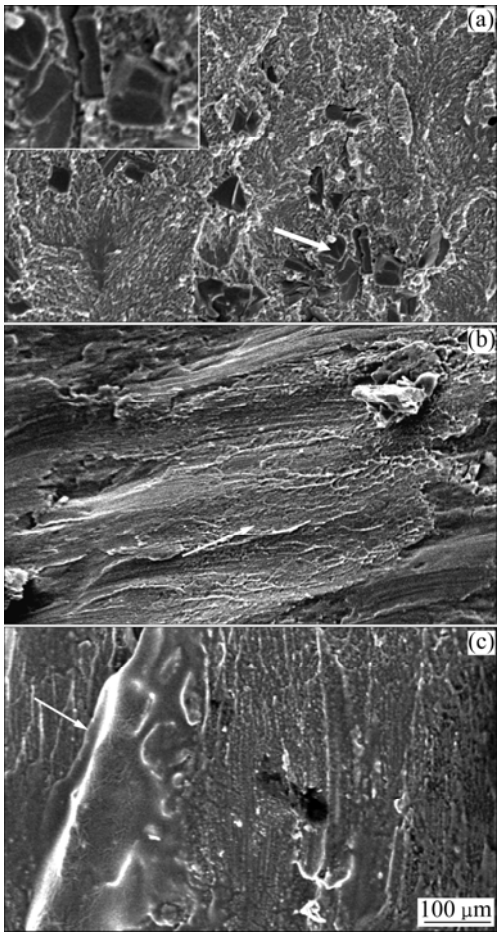

Fig.5 Microscopic fracture surfaces of $Dy_{65}(Fe_{0.6}Al_{0.4})_{35}$ (a) and $Dy_{70}(Fe_{0.6}Al0.4)_{30}$ (b, c)

cause the matrix to show more distinct viscous flow. The fracture surface of $Dy_{75}(Fe_{0.6}Al_{0.4})_{25}$ is similar to that of $Dy_{70}(Fe_{0.6}Al_{0.4})_{30}$.

4 Discussion

4.1 Forming mechanism of composites

It is well known that lowering the liquidus temperature, altering the alloy composition up to the eutectic or near the eutectic and increasing the number of components in the alloy are key steps in fabricating BMGs. Dy-Fe binary system has a binary eutectic point at composition $Dy_{71.8}Fe_{28.2}$ with T_E of 1 063 K. As the addition of Al has little influence on the binary eutectic point, the ternary $Dy_x(Fe_{0.6}Al_{0.4})_{100-x}$ (x=65, 70, 75) alloys reported in this work were developed based on this binary eutectic composition. Thus, the structure of the liquid of the $Dy_x(Fe_{0.6}Al_{0.4})_{100-x}$ alloys is more stable than that of the ternary Dy-Fe-Al alloys away from the binary eutectic point. And stabilized liquid phase to low temperature favors the formation of the gassy matrix of the $Dy_x(Fe_{0.6}Al_{0.4})_{100-x}$ alloys. During the solidification of these three alloys, the β-Dy phase at high temperature precipitates at first, then most of the phases transform to α-Dy phase. The content of the Dy phase in $Dy_x(Fe_{0.6}Al_{0.4})_{100-x}$ increases with the increase of the value of x, the content of Dy. As a result, there are more Dy phase precipitating in $Dy_{70}(Fe_{0.6}Al_{0.4})_{30}$ and $Dy_{75}(Fe_{0.6}Al_{0.4})_{25}$ but less in $Dy_{65}(Fe_{0.6}Al_{0.4})_{35}$. As there is strong bonding between Fe and Al due to more content of Fe and Al in the $Dy_{65}(Fe_{0.6}Al_{0.4})_{35}$, the ternary DyFeAl intermetallic is formed in the $Dy_{65}(Fe_{0.6}Al_{0.4})_{35}$ after combining Dy atoms.

4.2 Deformation and fracture mechanism of composites

The fracture of amorphous alloy takes place by inhomogeneous shear sliding accompanied by the generation of smooth regions on the surface, followed by an adiabatic failure at an applied stress level, which agrees with the fracture load at the reduced cross section caused by the shear sliding[12]. Fracture occurs along the maximum shear stress plane, which is inclined at 45° to the direction of compressive loading. As the deformation of the amorphous alloy concentrates on one or several shear bands and the other shear bands do not experience much deformation, unceasing deformation occurs and promotes further work-softening in one or several shear bands, finally leading to high fracture strength and catastrophic failure without obvious plastic strain and retaining a fracture surface consisting of a well-developed vein pattern and molten droplets. The phenomenon is attributed to local softening or melting induced by the decrease of viscosity or local adiabatic heating within the shear band[13−14].

For amorphous matrix composites including dendritic or crystalline particles, the dendritic or crystalline particles significantly affect the mechanical properties, the deformation and fracture mode of the material, depending on the nature, size, volume fraction and distribution. The broken ternary AlFeDy phase observed in the fracture surfaces of $Dy_{65}(Fe_{0.6}Al_{0.4})_{35}$ indicates that the phase is brittle as it belongs to intermetallic crystallites and does not yield large loading. Although the volume fraction of the phase in the composite is small, when small uniaxial compression loading exerts on the sample of the material, the phase first cracks due to the absence of plastic deformation such as dislocation motion and twinning and low fracture strength. Consequently, the stress intensity in the amorphous region bounded on the tip of cracks of the broken crystallites increases, rapid crack propagation takes place by spanning the tip and forms “penetrating crystalline cracks” (Fig.5(a)). These lead to the very low fracture strength of the whole composite (Fig.3), and the transformation of deformation and fracture mode from

shearing to cleavage (Fig.4(a)), which is similar to the embrittlement in the amorphous matrix composites including the quenched-in nanocrystals when the volume fraction of these nanocrystals is up to 10% although the size of the crystals is very small[15]. For $Dy_{70}(Fe_{0.6}Al_{0.4})_{30}$ and the $Dy_{75}(Fe_{0.6}Al_{0.4})_{25}$, the presence of the vein pattern, remelting on the fracture surface and fracture angle less than 45° indicates that the deformation and fracture behaviour of the two alloys are dominated by the shear fracture. However, the fracture surfaces are characterized by more viscous slurry-like flow layer (Fig.5(b)), and the larger liquid droplets (Fig.5(c)) are considered as severe remelting of the two alloys. These reveal that the dendritic phase, i.e. α-Dy dendrite embedded in the glassy matrix is not brittle due to its simple body cubic structure. It does not crack prematurely after yielding large loading, but retards the formation and the expansion of main shear band and increases the viscosity of its flow, resulting in the strengthening of the metallic glass, i.e. high fracture strength. Many in-situ dendrites or crystalline particles such as in-situ Ti-Zr-Nb β-phase primary dendrites[7] and in-situ Ta particles[16] can toughen metallic glass and make it have some even large plastic strain. But the present α-Dy dendrites in the two composites do not. This may be attributed to the fact that the former is soft and ductile, and the plastic deformation in these phases contributes to the plastic strain and initiate shear bands. While the latter (α-Dy dendrites) is neither ductile nor brittle, and little plastic deformation occurs in the dendrites, but they may have high yield and fracture strength, which results in the high fracture strength and shearing deformation and fracture mode of $Dy_{70}(Fe_{0.6}Al_{0.4})_{30}$ and $Dy_{75}(Fe_{0.6}Al_{0.4})_{25}$ consisting of the α-Dy dendrites and the glassy matrix.

In order to investigate the nature of AlFeDy intermetallic crystallite in $Dy_{65}(Fe_{0.6}Al_{0.4})_{35}$ and the α-Dy dendrites in $Dy_{70}(Fe_{0.6}Al_{0.4})_{30}$, an indentation experiment was carried out. Fig.6 shows the indented surfaces of the two alloys. A permanent deformation is observed in two cases. In the case of $Dy_{65}(Fe_{0.6}Al_{0.4})_{35}$, the radial cracks can be observed at the four corners of the indent though the amount of AlFeDy intermetallic crystallite in the alloy is little. While no crack can be observed in the indent pattern of $Dy_{70}(Fe_{0.6}Al_{0.4})_{30}$ though the amount of α-Dy dendrites in the alloy is high. This is a further indication that AlFeDy intermetallic crystallites are brittle and the α-Dy dendrites are not brittle.

The results and discussion above strongly suggest that for in-situ crystallite reinforced Dy-Fe-Al amorphous matrix composites, the nature (type) of in-situ crystalline phases embedded in the amorphous matrix has more important influence on the mechanical properties, the deformation and fracture behavior of the composites than other factors such as volume fraction and size.

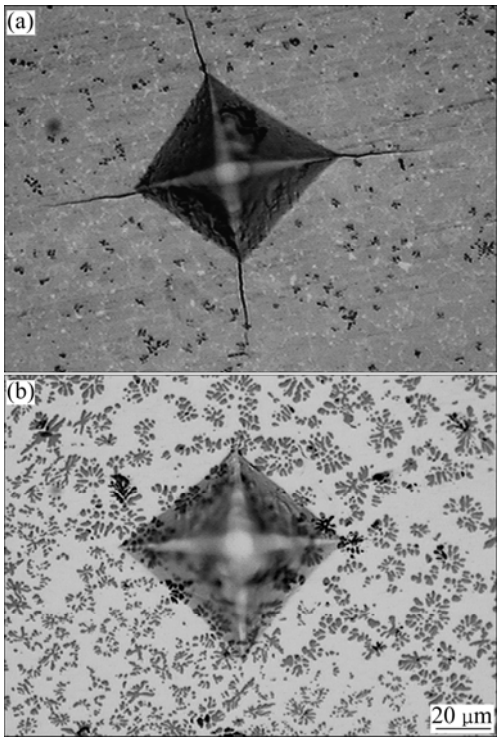

Fig.6 Indentation impressions of $Dy_{65}(Fe_{0.6}Al_{0.4})_{35}$ (a) and $Dy_{70}(Fe_{0.6}Al_{0.4})_{30}$ (b)

5 Conclusions

1) In-situ dendritic reinforced Dy-Fe-Al amorphous matrix composites with a diameter of 3 mm were fabricated by conventional Cu-mold casting method. The composites exhibit high fracture compressive strength and the strength of $Dy_{70}(Fe_{0.6}Al_{0.4})_{30}$ reaches 1 063 MPa.

2) The microstructures of the composites consist of many flower-like α-Dy dendrites and a few β-Dy particles embedded in a glassy matrix for $Dy_{70}(Fe_{0.6}Al_{0.4})_{30}$ and $Dy_{75}(Fe_{0.6}Al_{0.4})_{25}$, net-like ternary AlFeDy intermetallics and β-Dy particles for $Dy_{65}(Fe_{0.6}Al_{0.4})_{35}$, respectively.

3) The mechanical properties, the deformation and fracture behavior of the composites are affected mainly by the nature of in-situ crystalline phases embedded in the amorphous matrix. Although all three composites display an initial elastic deformation behavior with almost no plasticity at room temperature, $Dy_{65}(Fe_{0.6}Al_{0.4})_{35}$ containing brittle AlFeDy inter-metallics exhibits low strength, cleavage under compressive loading and the fracture surface of a brittle features with some broken crystals dispersing in a rough rock-layer matrix. While high strength, shear sliding and

the vein pattern and remelting on the fracture surface are the characteristic of $Dy_{70}(Fe_{0.6}Al_{0.4})_{30}$ and $Dy_{75}(Fe_{0.6}Al_{0.4})_{25}$ containing no-brittle α-Dy dendrites.

4) The different bearing-load ability of the in-situ crystalline phases embedded in the amorphous matrix results in the different mechanical properties, deformation and fracture behavior of the three composites.

References

[1] INOUE A, ZHANG T, MASUMOTO T. Production of amorphous cylinder and sheet of $La_{55}Al_{25}Ni_{20}$ alloy by a metallic mold casting method [J]. Mater Trans, 1990, 31(5): 425−431.

[2] HE Y, PRICE C E, POON S J. Formation of bulk metallic glass in neodymium-based alloys [J]. Phil Mag Lett, 1994, 70(6): 371−377.

[3] ZHANG T, INOUE A, CHEN J S. Amorphous $(Zr\text{-}Y)_{60}Al_{15}Ni_{25}$ alloys with two supercooled liquid regions [J]. Mater Trans, 1992, 33(2): 143−145.

[4] LEE M L, LI Y, SCHUH C A. Effect of a controlled volume fraction of dendritic phases on tensile and compressive ductility in La-based metallic glass matrix composites [J]. Acta Mater, 2004, 52(3): 4121−4131.

[5] TAN H, ZHANG Y, MA D, FENG Y P, LI Y. Optimum glass formation at off-eutectic composition and its relation to skewed eutectic coupled zone in the La based La-Al-(Cu, Ni) pseudo ternary system [J]. Acta Mater, 2003, 51(7): 4551−4561.

[6] INOUE A, ZHANG T, TAKEUCHI A. Hard magnetic bulk amorphous Nd-Fe-Al alloys of 12mm in diameter made by suction casting [J]. Mater Trans, 1996, 37(4): 636−640.

[7] HAYS C C, KIM C P, JOHNSON W L. Microstructure controlled shear band pattern formation and enhanced plasticity of bulk metallic glasses containing in situ formed ductile phase dendrite dispersion [J]. Phys Rev Lett, 2000, 84(14): 2901−2903.

[8] MA H, XU J, MA E. Mg-based bulk metallic glass composites with plasticity and high strength [J]. Appl Phys Lett, 2003, 83(14): 2973−2975.

[9] CHOI-YIM H, CONNER R D, SZUECS F, JOHNSON W L. Processing, microstructure and properties of ductile metal particulate reinforced $Zr_{57}Nb_5Al_{10}Cu_{15.4}Ni_{12.6}$ bulk metallic glass composites [J]. Acta Mater, 2002, 50(19): 2737−2745.

[10] KÜHN U, ECKERT J, MATTERN N, SCHULTZ L. ZrNbCuNiAl bulk metallic glass matrix composites containing dendritic bcc phase precipitates [J]. Appl Phys Lett, 2002, 80(16): 2478−2481.

[11] TAN H, ZHANG Y, LI Y. Synthesis of La-based in-situ bulk metallic glass matrix composite [J]. Intermetallics, 2002, 10(8): 1203−1205.

[12] CHEN H S, LEAMY H J, BARMA T Z. The elastic and anelastic behavior of a metallic glass [J]. J Non-Cryst Solids, 1971, 5(5): 444−448.

[13] STEIF P S, SPAEPEN F. HUTCHINSON J W. Strain localization in amorphous metals [J]. Acta Metall, 1982, 30(2): 447−455.

[14] OCELIK V, CSACH K, KASARDOVA A, BENGUS V Z. Anelastic deformation processes in metallic glasses and activation energy spectrum model [J]. Mater Sci Eng A, 1997, 226/228(15): 851−855.

[15] BIAN Z, CHEN G L, HE G, HUI X D. Microstructure and ductile-brittle transition of as-cast Zr-based bulk glass alloys under compressive testing [J]. Mater Sci Eng A, 2001, 316: 135−144.

[16] HUFNAGEL T C, CANG F, OTT RT. Controlling shear band behavior in metallic glasses through microstructural design [J]. Intermetallics, 2002, 10(4): 1163−1166.

(Edited by YUAN Sai-qian)